(Figure 6A and ref 30) contains a very narrow resonance at −48 ppm.[30] The additional sideband features present in Figure 6B arise, we believe, from the satellite ($\pm^1/_2 \leftrightarrow \pm^3/_2$; $\pm^3/_2 \leftrightarrow \pm^5/_2$) transitions. Similar results are predicted for the basic beryllium and zinc acetates and for the μ_6-oxo atoms in the $V_{10}O_{28}^{6-}$ ion. Such predictions are borne out for O_A (see, e.g., ref 31 for nomenclature) in the $V_{10}O_{28}^{6-}$ ion, as shown in Figure 6.

In Figure 6C we show the spectrum of the $V_{10}O_{28}^{6-}$ ion in H_2O solution, and the integrated peak intensities are as expected:[31] O_A (2), O_B (4), O_C (8), O_D (2), O_E (4), O_F (4), and O_G (4). All lines are quite narrow, except for $O_{F,G}$ which show partially resolved splittings, presumably due to $^1J_{^{51}V-^{17}O}$ interactions. In the crystalline solid state (as the Cs salt rather than the NH_4^+ salt to reduce dipolar interactions) the overall spectrum is, however, quite different, Figure 6D. The μ_6-oxo atom (O_A) has a very similar chemical shift (52.0 ppm) to that observed in solution (63.3 ppm). This result is consistent with the observation of a very sharp solution line width for O_A[31] (Figure 6C) and simply indicates a very high symmetry O^{2-} environment, as in the case of the Zn_4O(dtp) species (Figure 6B). However, the only other resonance in the solid-state ^{17}O NMR spectrum of $Cs_6V_{10}O_{28}$ to clearly correspond to the solution-state chemical shift and line width is that of O_B, the μ_3-O site. The more complex features of the $Cs_6V_{10}O_{28}$ spectrum will be discussed in more detail elsewhere.[32]

Concluding Remarks. The results presented in this paper represent our first attempts at obtaining and interpreting the ^{17}O solid-state NMR spectra of a variety of oxides an oxyanions, which we have carried out in order to provide a basis for further studies of related systems of catalytic and geochemical interest. Our results indicate that a very wide range of quadrupole coupling, chemical shift, and chemical shift anisotropy values are to be expected for ^{17}O nuclei in solids. We have presented results which indicate that species more covalent than silica (Si–O–Si) are unlikely to be amenable to investigation with either ^{17}O MASS or VASS NMR techniques with currently available magnetic field strengths. For the silicates themselves, however, even modest increases in magnetic field strengths (e.g., 500 → 600 MHz ^1H resonance frequency) will provide very significant (~50%) increases in spectral resolution, since for such systems resolution improves *quadratically* with increasing magnetic field strength.[3,4,11]

Our results with the simple SiO_4^{4-} and WO_4^{2-} species illustrate the potential power of solid-state ^{17}O NMR spectroscopy. Even in very simple oxyanions we have shown that nonequivalent oxygen atoms may be resolved, and that quadrupole coupling constants, chemical shift tensors, and their asymmetry parameters may be determined. Our results indicate that very large chemical shift anisotropies (some 300 ppm) are observed with some oxyanions (which also have vanishingly small e^2qQ/h values), and our unpublished results on metal carbonyls[33] indicate that $\Delta\sigma$ values as large as 600 ppm are to be expected for some species. We thus believe that the results presented in this publication indicate a very promising future for ^{17}O solid-state NMR studies in chemistry and geochemistry, especially for the structural analysis of systems not readily investigated by single-crystal X-ray diffraction techniques, by means of future detailed analyses of solid-state chemical shift and quadrupole coupling constant information.

Acknowledgment. We thank R. F. Bridger of the Mobil Research and Development Corporation, Princeton, NJ, for the sample of ^{17}O-labeled $Zn_4O(dtp)_6$, R. J. Kirkpatrick, for the sample of ^{17}O-labeled forsterite, and D. M. Henderson and R. J. Kirkpatrick for useful discussions. This work was supported in part by NIH, NSF, the American and Illinois Heart Associations, and the Mobil Foundation, by an Arnold O. Beckman Research Award from the University of Illinois, and has also benefitted from facilities made available through the University of Illinois–National Science Foundation Regional NMR Instrumentation Facility.

Registry No. ^{17}O, 13968-48-4; B_2O_3, 1303-86-2; $CaMgSi_2O_6$, 14483-19-3; Mg_2SiO_4, 15118-03-3; Al_2O_3, 1344-28-1; ZnO, 1314-13-2; K_2WO_4, 7790-60-5; MgO, 1309-48-4; *N*-methylsyndone, 6939-12-4; tetrahydropyran, 142-68-7; xanthene, 92-83-1; tetrachlorohydroquinone, 87-87-6; 2,5-dichlorohydroquinone, 824-69-1; *p*-chlorophenol, 106-48-9; cristobalite, 14464-46-1; ice, 7732-18-5.

(31) Klemperer, W. G.; Shum, W. *J. Am. Chem. Soc.* **1977**, *99*, 3544.
(32) Schramm, S.; Oldfield, E., unpublished results.
(33) Keniry, M. A.; Shinoda, S.; Brown, T. L.; Oldfield, E, unpublished results.

Two-Dimensional Heteronuclear Chemical Shift Correlation Spectroscopy in Rotating Solids

James E. Roberts, Shimon Vega,† and Robert G. Griffin*

Contribution from the Francis Bitter National Magnet Laboratory, Massachusetts Institute of Technology, Cambridge, Massachusetts 02139. *Received September 22, 1983*

Abstract: Two-dimensional NMR methods for performing heteronuclear chemical shift correlation experiments in rotating solids are described. The general approach involves both homo- and heteronuclear decoupling during the evolution (t_1) period followed by a coherence transfer or mixing period (τ_{mix}) in which information is transferred between the spin reservoirs. During the detection (t_2) period heteronuclear decoupling is employed and the NMR signals are observed in the customary fashion. Several methods for coherence transfer are discussed, and it is concluded that the method of choice will likely be sample dependent. Three different classes of two-dimensional spectra will be observed in these experiments—containing sidebands in neither, one, or both spectral dimensions—and examples of each type are described. Finally, the occurrence of rotor frequency lines in multiple-pulse/magic-angle sample spinning ^1H spectra is discussed.

Introduction

Despite the availability of sophisticated pulse sequences that attenuate the proton–proton dipolar interaction,[1] the task of obtaining high-resolution proton spectra of polycrystalline powders remains difficult. The residual line widths obtained with multiple-pulse sequences during magic-angle sample spinning (MASS) are typically 2 ppm.[2-4] When compared to the normal 10–15-ppm

† On leave from the Isotope Department, Weizmann Institute of Science, Rehovoth, Israel.

(1) (a) Mehring, M. "High Resolution NMR in Solids", 2nd ed.; Springer-Verlag: Berlin, 1983. (b) Haeberlen, U. "High Resolution NMR in Solids, Selective Averaging"; Academic Press: New York, 1976.

0002-7863/84/1506-2506$01.50/0

Figure 1. General pulse sequence for two-dimensional solid-state heteronuclear chemical shift correlation experiments. The preparation period includes presaturation of the carbon spin reservoir and a 90_x pulse on the I spins. The t_1 evolution time contains a multiple-pulse sequence (MREV-8) with continued saturation of the S spins. The mixing period consists of one of the pulse sequences illustrated in Figure 2, and the detection (t_2) is performed with proton decoupling.

proton chemical shift dispersion, it is apparent that only four or five inequivalent proton signals are distinguishable in a given experiment. This fact severely constrains the types of samples amenable to analysis. A situation similar to this occurs in ^1H solution spectroscopy in that proton spectra of large molecules are rarely completely resolved.

There are a number of approaches involving two-dimensional (2D) techniques[5] which can be employed to increase spectral resolution. For example, in proton solution spectroscopy the Jeener experiment[6] and extensions of it have been used for this purpose.[5-7] More recently, 2D ^{13}C–^1H chemical shift correlation spectroscopy has been demonstrated to be very effective in increasing the resolution of proton spectra.[8] Although these experiments have been used primarily to study small molecules, they have recently been extended to the examination of a number of proteins.[9] The utility of correlation experiments arises because of the large spectral dispersion present in the ^{13}C dimension of the spectra.

In order to improve the resolution in solid-state proton spectra, we have applied two-dimensional heteronuclear chemical shift correlation techniques to carbon–proton systems during magic-angle sample spinning (MASS). The superior dispersion and resolution of the carbon chemical shifts effectively separates overlapping proton resonances in the second dimension. The overall proton resolution is improved substantially over conventional methods. The experiments discussed here are useful as assignment aids for both proton and carbon chemical shifts. In complicated molecules, this technique may help resolve overlapping rotational sideband patterns from inequivalent carbon atoms. The text is divided into sections discussing pulse sequences for 2D MASS correlation spectroscopy, coherence transfer in rotating solids, comparison of transfer characteristics, pure-phase experiments, 2D chemical shift correlation spectra in rotating solids, and finally, rotor frequency lines which occur during multiple-pulse/MASS experiments.

Pulse Sequences for Two-Dimensional MASS Correlation Spectroscopy

Two-dimensional chemical shift correlation experiments were performed in liquids some time ago,[8] and recently they have been extended to studies of single crystalline solids.[10] Here we incorporate MASS into the solid-state experiment.

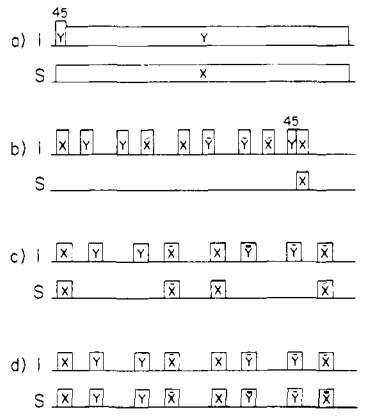

Figure 2. Pulse sequences employed for the coherence transfer during two-dimensional solid-state heteronuclear chemical shift correlation experiments: (a) mixing via cross polarization; (b) τ–90_I90_S–τ transfer with a MREV-8 cycle inserted in the first τ period; (c) MREV-8 pulsed cross polarization; (d) simultaneous MREV-8 cycles with cross polarization. See text for details.

The general Hamiltonian relevant to chemical shift correlation spectroscopy in solids is given in eq 1. The five major terms

$$\mathcal{H}_{ij} = -\sum_i \omega_i^I I_{zi} - \sum_j \omega_j^S S_{zj} - \sum_i \sum_j J_{ij}^{IS} I_{zi} S_{zj} - \sum_i \sum_j D_{ij}^{IS} I_{zi} S_{zj} - \sum_i \sum_j D_{ij}^{II}(3I_{zi}I_{zj} - I_i I_j) \quad (1)$$

represent the proton resonance offset and chemical shift (I spins), the carbon resonance offset and chemical shift (S spins), the heteronuclear proton–carbon scalar (J) coupling, the heteronuclear carbon–proton dipolar interaction, and the homonuclear proton–proton dipolar coupling, respectively. The constants J_{ij}^{IS} and D_{ij}^{IS} are the direct and indirect dipolar couplings appropriate for each term. Successful completion of a two-dimensional NMR experiment requires manipulation of this Hamiltonian to eliminate one or several of the terms during each time period. This procedure is illustrated below with the general pulse sequence used in solid-state chemical shift correlation spectroscopy.

The pulse sequences for all the experiments discussed here share many common properties, and a typical example is shown in Figure 1. The experiment begins with a preparation period which in this case involves presaturation of the S spins. This ensures that the S spin signals which are eventually detected arise from transferred coherence of the I spins, and not from equilibrium S spin magnetization. Concurrently, the I spins are initially excited with a 90° pulse and subsequently evolve during t_1 under the influence of a homonuclear decoupling pulse train, in our case, MREV-8. In addition, we have depicted the S spins as being decoupled during t_1. This is best accomplished in this inhomogeneously broadened case with composite pulses. However, on resonance continuous irradiation of the carbon spins will provide adequate heteronuclear decoupling provided the carbon irradiating field satisfies

$$2\pi/\omega_1^{^{13}C} = 2\tau/n \quad (2)$$

where n is an integer and τ is the small window of the multiple-pulse cycle.[1] If decoupling is not used during t_1 then scaled ^{13}C–^1H dipolar splittings will be present in the $\omega_1/2\pi$ dimension of the spectrum. The MREV-8[13,14] train dramatically attenuates ^1H–^1H dipolar coupling and scales the ^1H chemical shifts by $2^{1/2}/3$ during this period. The increment during t_1 is the cycle time of the MREV-8 sequence and is 12τ (typically 48 μs). The only interaction during t_1 is the scaled proton chemical shift and resonance offset.

The most substantial difference between the liquid- and solid-state experiments is the way in which the coherence transfer

(2) Taylor, R. E.; Pembleton, R. G.; Ryan, L. M.; Gerstein, B. C. *J. Chem. Phys.* **1979**, *71*, 4541.
(3) Ryan, L. M.; Taylor, R. E.; Paff, A. J.; Gerstein, B. C. *J. Chem. Phys.* **1980**, *72*, 508.
(4) Scheler, G.; Haubenreisser, U.; Rosenberger, H. *J. Magn. Reson.* **1981**, *44*, 134.
(5) Aue, W. P.; Bartholdi, E.; Ernst, R. R. *J. Chem. Phys.* **1976**, *64*, 2229.
(6) Jeener, J., Ampere International Summer School, Basko Polje, Yugoslavia, Sept 1, 1971.
(7) Nagayama, K.; Kumar, A.; Wuthrich, K.; Ernst, R. R. *J. Magn. Reson.* **1980**, *40*, 321.
(8) (a) Maudsley, A. A.; Müller, L.; Ernst, R. R. *J. Magn. Reson.* **1977**, *28*, 463. (b) Bodenhausen, G.; Freeman, R. *J. Magn. Reson.* **1977**, *28*, 471.
(9) Chan, T.-M.; Markley, J. L. *J. Am. Chem. Soc.* **1982**, *104*, 4010.
(10) Caravatti, P.; Bodenhausen, G.; Ernst, R. R. *Chem. Phys. Lett.* **1982**, *89*, 363.
(11) (a) Levitt, M. H.; Freeman, R. *J. Magn. Reson.* **1981**, *43*, 502. (b) Levitt, M. H.; Freeman, R.; Frenkiel, T. *Ibid.* **1982**, *47*, 328. (c) Levitt, M. H.; Freeman, R.; Frenkiel, T. *Ibid.* **1982**, *50*, 157.
(12) Shaka, A. J.; Keeler, J.; Frenkiel, T.; Freeman, R. *J. Magn. Reson.* **1983**, *52*, 335.
(13) Rhim, W. K.; Elleman, D. D.; Vaughan, R. W. *J. Chem. Phys.* **1973**, *59*, 3740.
(14) Mansfield, P.; Orchard, M. J.; Stalker, D. C.; Richards, K. H. B. *Phys. Rev. B: Condens. Matter* **1973**, *B7*, 90.

or mixing is performed during the period t_{mix} (represented by the cross-hatched area in Figure 1). The requirements are basically twofold. First, the transfer should be selective in that the S spins obtain coherence only from directly bonded I spins. Secondly, the transfer should be efficient so that the S spin signals are large. We will discuss these considerations in more detail below. Finally, the S spin signal is detected during t_2, while the I spins are being decoupled with continuous wave irradiation, leaving only the S spin resonance offset and chemical shift.

Coherence Transfer in Rotating Solids

A. Background. There are several well-known procedures whereby coherence transfer may be accomplished during the mixing period. These include cross polarization,[15] single-pulse transfers,[16,17] and multiple-pulse transfers or cross polarization.[18,19] These techniques are illustrated in Figure 2. Cross polarization (Figure 2a) is a simple and efficient means to transfer coherence between I and S spin reservoirs. Unfortunately, this procedure is generally nonselective, and the resolution in the ^1H dimension is lost. However, when strong heteronuclear dipolar coupling is present, short time cross polarization (i.e., ~ 20 μs) can be employed which is still selective. An example illustrating these points will be given below.

In solution ^{13}C–^1H spectra coherence transfer is accomplished via the heteronuclear J coupling.[8] The size of these couplings is known, and therefore a pair of pulses, one each at the ^1H and ^{13}C frequency, can be used to perform the transfer. In solution this technique is both selective and efficient. Figure 2b shows an analogous mixing sequence for spectroscopy of rotating solids. It begins with a period τ which is approximately equal to the reciprocal of the size of the interaction through which the transfer is accomplished—i.e., the CH dipolar coupling. During this period the spin diffusion among the I spins (usually protons) is quenched by application of a multiple-pulse train and then a pair of pulses is applied to the ^1H and ^{13}C spins. This process exhibits quite good selectivity; however, since it is selective for a narrow range of dipolar couplings present in a powder sample, the intensitites of the ^{13}C signals are well below that obtained with normal cross polarization.

Some time ago, Stoll et al.[18] suggested a means to partially circumvent this problem which is illustrated in Figure 2c. In this case the selectivity is maintained by the presence of the multiple-pulse train on the I spins, which suppresses the homonuclear I–I interactions, and the pulses on the S spins, which create an effective dipolar average Hamiltonian. Due to cross polarization during the x and $\bar{x}$ pulses of finite length in the MREV-8 cycle the efficiency of the polarization transfer is increased. The multiple-pulse train attenuates the proton–proton dipolar interactions sufficiently, but the heteronuclear dipolar coupling is only scaled by $2^{1/2}/3$. Thus, the carbon–proton dipolar interaction coupled with MASS attenuates the carbon polarization very rapidly, and the transfer efficiency is decreased significantly when more than one cycle is utilized.

Another alternative coherence-transfer method was recently suggested by Weitekamp et al.[19] and is illustrated in Figure 2d. Employing simultaneous multiple-pulse trains under cross-polarization conditions on both the I and S spin systems suppresses the proton–proton dipolar coupling and therefore gives good selectivity. Since the contact time is extended from Figure 2c the efficiency of the transfer is higher. Moreover, the multiple-pulse cycles may be repeated to obtain the maximum sensitivity. However, it must be noted that the longer cross-polarization times of this technique allow nonprotonated carbon signals to appear, although they are generally considerably weaker than lines arising from protonated carbon atoms.

(15) Pines, A.; Gibby, M. G.; Waugh, J. S. *J. Chem. Phys.* **1973**, *59*, 569.
(16) Morris, G. A.; Freeman, R. *J. Am. Chem. Soc.* **1979**, *101*, 760.
(17) Burum, D. P.; Ernst, R. R. *J. Magn. Reson.* **1980**, *39*, 163.
(18) Stoll, M. E.; Rhim, W.-K.; Vaughan, R. W. *J. Chem. Phys.* **1976**, *64*, 4808.
(19) Weitekamp, D. P.; Garbow, J. R.; Pines, A. *J. Chem. Phys.* **1982**, *77*, 2870.

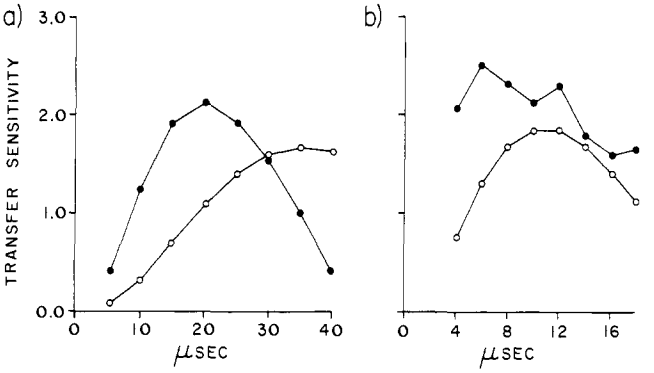

Figure 3. Calculated coherence transfer efficiencies for a CH_2 group from various mixing period pulse sequences: (a) τ–90_I90_S–τ transfer with heteronuclear dipolar coupling of 47 kHZ (●) and 22.1 kHz (○); (b) MREV-8 pulsed transfer (○) and simultaneous multiple-pulse cross polarization (●), C–H dipolar coupling = 22.1 kHz. The relative sensitivity is compared to a ^{13}C Bloch decay = 1.0. See text for discussion.

B. Comparison of Transfer Characteristics. As might be expected, the transfer efficiency of the various techniques discussed above depends critically on the timing parameters of the mixing period. We have calculated results expected for the pulse sequences in Figure 2b–d with a computer program to be described elsewhere.[20,21]

Briefly, the program divides the NMR experiment into a set of time intervals; within each interval the system evolves under a well-defined Hamiltonian. The system is described by a reduced equilibrium density matrix in the rotating frame

$$\rho(t_f) = U(t_i,t_f)\rho(t_i)U^+(t_i,t_f) \tag{3}$$

where $U(t_i,t_f)$ is the time evolution operator for the time period t_i to t_f

$$U(t_i,t_f) = \hat{T}\exp\left(-i\int_{t_i}^{t_f}\mathcal{H}(t')\,dt'\right) \tag{4}$$

and $\hat{T}$ is the Dyson time ordering operator. A complete simulation requires four steps: (1) calculation of the time evolution operator for each time interval by using the appropriate portion of the total Hamiltonian given in eq 1; (2) calculation of τ_N by using the time evolution operators; (3) sample τ_N at appropriate times to obtain a calculated FID; and (4) repeat steps 1–3 for different Euler angles to obtain a powder average.

The model system chosen was a CH group with chemical shift tensors −0.6, −0.6, and +1.2 kHz for the protons and −0.8, −0.8, and +1.6 kHz for the carbon, and 2.0 kHz was employed as a representative spinning speed. The heteronuclear dipolar coupling was assumed to be 47.0 or 22.1 kHz. These parameters approximate the CH_2 group in sodium propionate. All pulses are perfect δ-function 90° rotations of appropriate phase for the mixing technique. All calculations neglect proton–proton interactions, and initial carbon polarizations are zero (i.e., presaturation as in Figure 1). With these parameters, both proton and carbon spectra contain ≥90% of the integrated intensity in the centerband.

Figure 3a presents the calculated centerband coherence-transfer sensitivity for the τ–90_I90_S–τ technique (Figure 2b) as a function of τ. The two data sets represent heteronuclear dipolar couplings of 47.0 and 22.1 kHz. The sensitivity scale is relative to a simple 22.1-kHz ($47.0 \times 2^{1/2}/3$ (the MREV scaling factor)) Bloch decay experiment = 1.0 (i.e., perfect cross polarization $\simeq$ 4). Note the smaller dipolar coupling results in a longer τ value and less efficient transfer, suggesting this technique is only feasible for strongly coupled systems (but see below). The "MREV-8 pulsed" (Figure 2c) and simultaneous MREV-8 cross-polarization (Figure 2d) calculation results are shown in Figure 3b. Interestingly, the plots show that quantitatively all three methods yield about the same

(20) Olejniczak, E. T.; Vega, S.; Griffin, R. G. *J. Chem. Phys.*, submitted for publication.
(21) Vega, S.; Olejniczak, E. T.; Griffin, R. G. *J. Chem. Phys.*, in press.

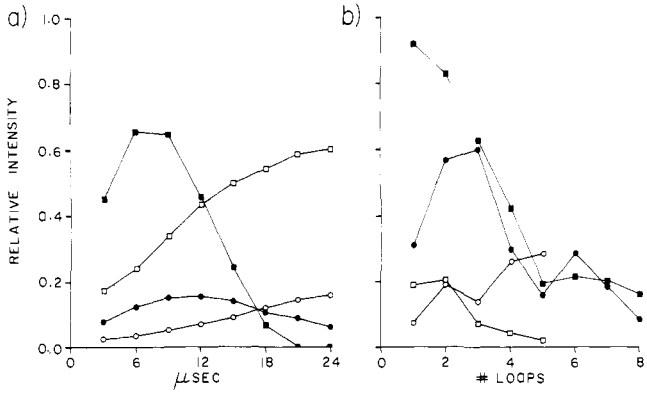

Figure 4. Experimental determination of coherence-transfer sensitivity for the methyl and methylene groups of sodium propionate. The reference intensity is 1.0 for each centerband, obtained with 3-ms cross polarization: (a) intensity vs. time for cross polarization (□), CH_2, (○) CH_3) and τ-90_I90_S-τ without MREV-8 ((■) CH_2, (●) CH_3); (b) intensity vs. number of MREV-8 cycles for MREV-8 pulsed transfer ((□) CH_2, (○) CH_3) and simultaneous MREV-8 cross polarization ((■) CH_2, (●) CH_3). See text for details.

size carbon polarization. Specifically, these three techniques are within 30% of each other in terms of overall transfer efficiency. However, we emphasize that these calculations were performed with perfect δ-function pulses and varying τ between the pulses, in addition to assuming no I–I coupling. In contrast, the actual experiments are performed under Hartmann–Hahn matched cross-polarization conditions (Figures 2c,d and 3b), and both cross polarization and multiple-pulse transfer analogous to the τ-90_I90_S-τ sequence could be active in producing the observed response.

To compare the calculations with experiment, we have examined the coherence-transfer sensitivity of the pulse sequences in Figure 2a–d by using sodium propionate as a prototype hydrocarbon. All data was obtained for $t_1 = 0$ with presaturation of the carbon spins. The proton resonance offset was $\sim$−3 kHz; the carbon offsets were 0 and $\sim$−1.5 kHz for the CH_2 and CH_3 groups, respectively. Figure 4a demonstrates the sensitivity dependence on mixing time for cross-polarization and τ-90_I90_S-τ-pulsed transfer without a MREV-8 cycle during the first τ period. Both techniques give smoothly varying curves, and the intensity vs. time behavior is continuous, as expected. The carbon centerband intensities are compared to those obtained with standard cross polarization of 3.0 ms. Both techniques are reasonably selective; none of these spectra contained significant carbonyl signal intensity. As the calculations suggested, the τ-90_I90_S-τ transfer yields acceptable signal strengths for the methylene group, but the smaller heteronuclear dipolar coupling of the methyl group results in reduced signal strengths, and the technique is therefore of limited utility for this type of group. We note the experiment allows homonuclear coupling during τ; for this reason the maximum sensitivities are not obtained at the same value of τ for the calculations and the experiment.

Figure 4b presents similar data obtained with MREV-8 pulsed and simultaneous MREV-8 multiple-pulse cross polarization (Figure 2c,d). The time interval for this plot is that of one multiple-pulse cycle, 48 μs. Again, the calculations predicted the correct relative sensitivities, although cross polarization was not included in the calculations. The simultaneous multiple-pulse cross-polarization transfer is sufficiently sensitive that experiments on natural abundance materials become feasible. It is also important to note that both CH_2 and CH_3 are readily observed with this technique. As the number of MREV-8 loops goes up, the carbonyl lines also appear in the carbon spectrum, although they remain below 20% of the intensity obtained with cross polarization for 3.0 ms. In principle, the position of these weak lines in the proton dimension yields information about the cross-polarization mechanism (vide infra).

The various transfer techniques discussed here vary dramatically in efficiency of coherence transfer (see Figure 4). There are two principle reasons for this variability. First, it is important to realize that in polycrystalline powders, there is a distribution of tensor values. For example, the heteronuclear dipolar interactions in the methylenes of a sample vary from +47 to −23.5 kHz, depending on the orientation of the individual crystallite with respect to the static magnetic field. If the transfer sequence is optimized for one orientation, it is not well adjusted for many others. For short-time cross-polarization and τ-pulsed transfer, this in itself is a sufficient explanation for their observed low sensitivities.

The MREV-8 pulsed transfer (Figure 2c) suffers from the same problem in a different way. The actual transfer is accomplished through small periods of cross polarization. A complicating factor is the heteronuclear dipolar interaction—it does not vanish over the cycle. Thus there are two competing effects: cross polarization at short contact times that favor transfer for those molecules in an orientation with a large dipolar coupling and the nonvanishing dipolar coupling itself, which rapidly attenuates the carbon signal amplitude during MASS. For methyl groups, molecular motion partially averages the dipolar interaction. In fact, CH_3 sensitivity actually *increases* as the number of MREV-8 cycles is repeated, until other factors dominate. In this manner it is possible to selectively observe only weakly coupled systems (i.e., methyl groups).

Simultaneous multiple-pulse cross polarization does not sufer from this problem. Specifically, the heteronuclear dipolar coupling remains constant over a properly adjusted sequence, and cross-polarization time can be much longer than that for either normal short-time cross polarization or MREV-8 pulsed transfer. This increases sensitivity but also in principle limits the selectivity. Although proton–proton communication is virtually eliminated by the proton MREV-8 cycle, the longer cross-polarization contact time allows nonbonded coherence transfer. For example, the nonprotonated carbonyl carbon of sodium propionate gives rise to a weak signal, indicating cross polarization from the nearby methylene protons. In principle, this technique allows correlating unprotonated carbon atoms with nearby protons and therefore nearby carbon atoms.

The second factor affecting sensitivity applies to all the transfer techniques. Each mixing period requires a finite fraction of a spinner period during which time the individual crystallites change orientation with respect to the field. This implies an alteration of the heteronuclear dipolar interaction, leading to a lower sensitivity in general. For example, in the τ-pulsed transfer, a given crystallite might be suitably oriented for optimal preparation during the first period but has changed positions for the second one. This general phenomenon may not be very important because in most cases the mixing time is only 5–10% of a rotor period.

C. Pure-Phase Experiments. Two of the above procedures transfer only one component of the proton magnetization to the S spins during the mixing period. For these pulse sequences (Figures 2a,b) it is possible to perform pure-phase experiments.[22,23] The advantages of a pure-phase presentation over the conventional absolute magnitude spectrum are twofold: line widths are $2^{1/2}$ smaller in the pure-phase experiment and peak tails are drastically reduced. Both factors lead to an effective resolution enhancement for the pure-phase display compared to an absolute magnitude spectrum. The main disadvantages are the $2^{1/2}$ smaller signal-to-noise ratio obtained in a given time and the necessity of performing two separate experiments with appropriate data manipulation.

To obtain pure-phase data, the real and imaginary components of the t_1 dimension are obtained in two separate experiments with phase cycling. The two free-induction decays for each t_1 value are stored and Fourier transformed separately. After phase correction (appropriate for $t_1 = 0$), the complex time domain data for t_1 is assembled from the extracted real parts of the two complex frequency domain spectra for each t_1 value. The resulting complex

(22) Bachmann, P.; Aue, W. P.; Müller, L.; Ernst, R. R. *J. Magn. Reson.* **1977**, *28*, 29.
(23) States, D. J.; Haberkorn, R. A.; Ruben, D. J. *J. Magn. Reson.* **1982**, *48*, 286.

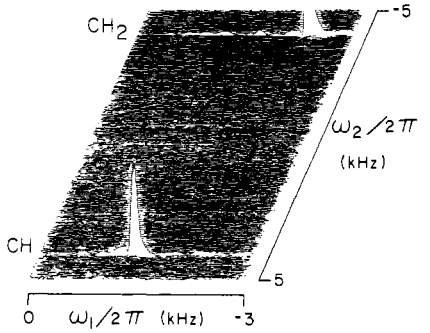

Figure 5. Heteronuclear chemical shift correlation MASS spectrum of natural abundance *cis*-polybutadiene obtained with the τ–90_I90_S–τ-pulsed transfer (Figure 2b, τ = 1 ms). No multiple-pulse cycles were required because the rapid chain reorientation averages the I–I interaction efficiently.

matrix is transposed and Fourier transformed to give the final pure-phase 2D spectrum. Phase correction may be applied in the ω_1 dimension, although none is usually required. Note that proper phase cycling and combination of spectra automatically yields quadrature detection in both frequency domains.[23]

Two-Dimensional Chemical Shift Correlation Spectra in Rotating Solids

A. Background. Heteronuclear chemical shift correlation spectra can be divided into three general categories. The first includes spectra that exhibit only centerbands in both dimensions. This case is observed in ^{13}C–^1H spectra in the limit of low fields (i.e., ^1H at 60 MHz) and/or fast spinning rates or, as will be seen below, when fast motion partially averages the chemical shift tensors. The second category consists of spectra with rotational sidebands in one dimension and isotropic shifts alone in the second. Such cases are commonly encountered in ^{13}C–^1H spectra obtained at currently available operating fields and spinning speeds, e.g., ^1H at 200–400 MHz, $2 < \nu_R < 5$ kHz. Generally, sidebands appear in the ^{13}C but not in the ^1H dimension. The third category will be encountered in experiments at higher magnetic fields (>500 MHz), where ^{13}C–^1H spectra can be expected to exhibit rotational sidebands in both dimensions. In addition, spectra of other spin pairs where both members have large shift anisotropies—e.g., ^{13}C–^{15}N—will also exhibit this type of spectrum. In this section we discuss these three general cases, presenting data for the first two and predictions for the third. Finally, we discuss the phenomenon of rotor frequency lines which arise from interaction of the multiple-pulse train and the sample rotation.

B. Isotropic Spectra in Both Spectral Dimensions. Figure 5 presents the heteronuclear MASS chemical shift correlation spectrum of *cis*-polybutadiene. Although it is a solid, this rubberlike compound is considered a "pseudosolid" because it exhibits rapid chain motion at room temperature. As a consequence, both the proton and carbon MASS spectra consist of two single lines arising from CH and CH_2 groups.[24] The spectrum shown in Figure 5 was obtained by using the τ–90_I90_S–τ-pulsed transfer (Figure 2b) without any MREV-8 cycles, in direct analogy to solution studies. The clearly separated lines and excellent selectivity confirm the feasibility of the experiment during MASS on isotropic systems.

cis-Polybutadiene is clearly an example of the centerbands only case. The rapid chain motion significantly averages the chemical shift tensors of both the carbon and hydrogen atoms. In carbon MASS spectra obtained without proton decoupling, a doublet and triplet appear yielding ^{13}C–^1H J couplings of ~127 and ~153 Hz for the CH_2 and CH groups.[24] The lack of rotational sidebands (MASS at 2.5 kHz) in all spectra indicates the heteronuclear dipolar interaction is significantly reduced by the motion as well. The well-resolved proton resonance spectrum obtained with MASS demonstrates the I–I dipolar interaction is also small, and for these reasons, we applied solution NMR techniques to obtain the spectrum in Figure 5. In particular, we found that good coherence transfer could be accomplished with the τ–90_I90_S–τ method with τ = 1.0 ms, which is on the initial slope curve for this technique.[17] In analogy to solution studies, the optimal transfer time is expected to be $^1/_2J \simeq 3.8$ ms for the observed J couplings of *cis*-polybutadiene. The detailed behavior of the transfer dependence on τ suggests that reasonable sensitivity is obtained with many times; i.e., changes of only 0.2 ms in τ can cause the complete disappearance of one or the other of the carbon lines. This results from an interdependence of the J coupling, the small heteronuclear dipolar interaction, and the proton resonance offsets, any of which could significantly alter transfer characteristics for a single set of phase settings. Utilizing a pure-phase experiment eliminates the proton resonance offset dependence of transfer sensitivity but lowers the overall sensitivity by a factor of $2^{1/2}$. Nevertheless, the results of Figure 5 demonstrate this technique can successfully be employed on systems with considerable motion.

The "centerbands only" category of spectra may be more prevalent than one might think. Certain pathological cases such as adamantane and camphor fall into this category,[25] as will any other system with fast, reasonably isotropic molecular motion—e.g., liquid crystalline systems such as lipid dispersions or membrane proteins.[26] It is worth noting that in these cases the resolution in the proton dimension is quite good—e.g., in the *cis*-polybutadiene spectra of Figure 5 the ^1H line widths are ~0.1 ppm. Finally, it is in principle possible to incorporate chemical shift scaling into one or both of the spectral dimensions.[27,28] In such a case, any sidebands present could be scaled to essentially zero, resulting in a "centerbands only" class of two-dimensional spectrum.

C. Rotational Sidebands in One Dimension. Sodium propionate and *p*-dimethoxybenzene (PDMB) represent the second general category of spectral types with sidebands in the carbon dimension. There are five general types of carbon atoms of interest: CH_3, CH_2, CH, aromatic CH, and nonprotonated carbon groups. At $\nu_{^{13}C}$ = 80 MHz and MASS at 2–3 kHz, the sidebands of both CH_3 and CH_2 carbon atoms are fairly small (~10% integrated intensity), while CH, aromatic, and quaternary carbon signals typically contain several rotational sidebands which can be used to extract shift anisotropies.[29]

Sodium propionate (30% ^{13}C) was examined with all the transfer techniques discussed above. Stacked plots obtained with cross polarization during the mixing period are shown in Figure 6. The contact times were (a) 3.0 ms and (b) 20 μs. At long contact times (Figure 6a), excellent sensitivity is obtained, but the selectivity has vanished. Not only are the carbonyl resonances present but all proton domain resonances appear at the same frequency in the ω_1 dimension. In contrast, the short contact times ($\leq$25 μs) yield much poorer signal-to-noise ratios but resolve the ~1-ppm chemical shift separations between proton signals from CH_2 and CH_3 groups. Although this resolution is not very apparent in the stacked plot of Figure 6b, it is easily discerned in the contour plot of the same data presented in Figure 7. The contour plot also emphasizes the ability to detect even weak rotational sidebands.

In addition to the increased resolution of the short cross-polarization contact time, the selectivity is enhanced as the nonprotonated COO^- moiety resonances are greatly suppressed. All the transfer methods of Figure 2 gave substantially the same results as those shown in Figure 6b for sodium propionate, although the

(24) English, A. D.; Dybowski, C. R., presented in part at the 24th Experimental NMR Conference, Asilomar, CA, 1983.

(25) Terao, T.; Miura, H.; Saika, A. *J. Am. Chem. Soc.* **1982**, *104*, 5228.
(26) Haberkorn, R. A.; Herzfeld, J.; Griffin, R. G. *J. Am. Chem. Soc.* **1978**, *100*, 1297.
(27) Aue, W. P.; Ruben, D. J.; Griffin, R. G. *J. Magn. Reson.* **1982**, *46*, 354.
(28) Aue, W. P.; Ruben, D. J.; Griffin, R. G. *J. Chem. Phys.* **1984**, *80*, 1729.
(29) Herzfeld, J.; Berger, A. E. *J. Chem. Phys.* **1980**, *73*, 6021.

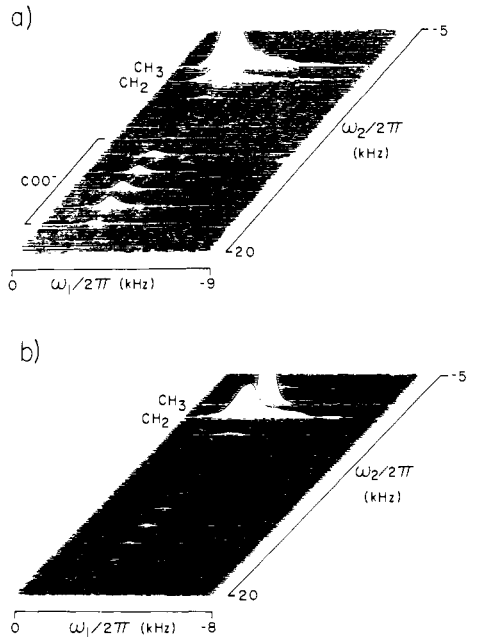

Figure 6. Stacked plots of 30% ^{13}C-enriched sodium propionate heteronuclear chemical shift correlation data obtained with cross-polarization contact times of (a) 3.0 ms and (b) 20 μs. For long contact times, selectivity vanishes and all proton frequencies are identical. The short contact time in b suppresses the nonprotonated resonances; the chemical shift difference between methyl and methylene proton lines is now apparent.

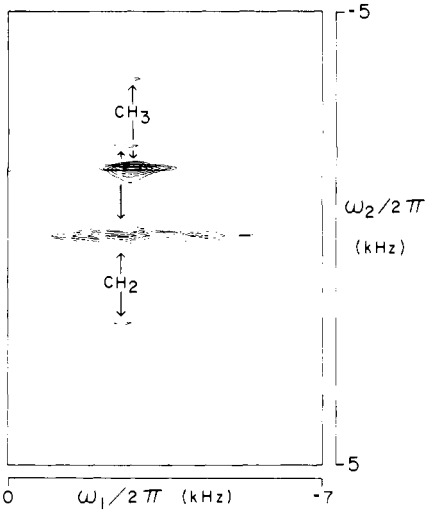

Figure 7. Contour plot of the aliphatic region of data in Figure 6b. The ~1 ppm separation of the CH_3 and CH_2 proton resonances is readily apparent, demonstrating the increased proton resolution obtainable with two-dimensional heteronuclear chemical shift correlation spectroscopy. Contours start at 0.03 and increase by factors of 2.

sensitivity of the various procedures varied considerably as discussed above.

To demonstrate the feasibility of the heteronuclear chemical shift correlation experiment on natural abundance polycrystalline powders, Figure 8 presents a contour plot of data from PDMB obtained with simultaneous multiple-pulse cross polarization (Figure 2d). The aromatic proton peak positions are well separated from the methoxy ^1H resonances, as expected. These results allow unambiguous determination of the proton chemical shifts in this compound; conventional one-dimensional multiple-pulse measurements during MASS show only a semiresolved shoulder from the aromatic protons. In addition, the nonprotonated aromatic carbon peaks are suppressed to ~25% of the protonated ones. The observation of nonprotonated aromatic carbon resonances is in

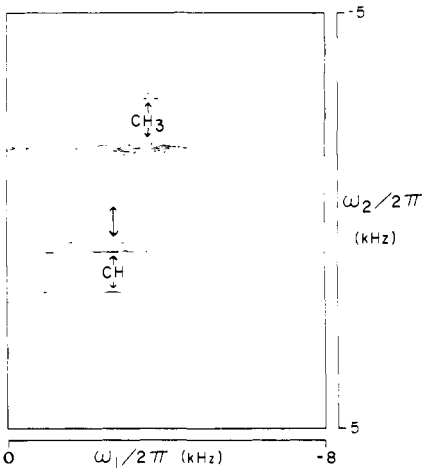

Figure 8. Contour plot of a natural abundance *p*-dimethyoxybenzene spectrum obtained with simultaneous MREV-8 cross polarization (Figure 2d). The aromatic and methoxy ^1H positions are well separated; in addition, the nonprotonated aromatic carbon signals are significantly suppressed. Contours are at 0.09, 0.18, 0.36, and 0.72.

agreement with the prediction that this transfer technique allows observation of all resonances, in principle. The suppression is achieved by limiting the total contact time to only one or two multiple-pulse cycles. We also note the proton position correlated with a nonprotonated carbon resonance allows indirect determination of spin diffusion among the protons. For PDMB, all aromatic carbon peaks are cross polarized from the aromatic protons, and not from the methoxy groups.

When ^{13}C rotational sidebands overlap, correlation with proton chemical shifts can help unravel the carbon chemical shift tensors. When coupled with other spectral simplification techniques, such as chemical shift scaling,[27,28] two-dimensional chemical shift correlation experiments could be a valuable aid in assigning resonance from polycrystalline solids. The same is true in reverse, namely proton assignments can be made using the superior ^{13}C chemical shift dispersion.

D. Rotational Sidebands in Both Dimensions. Two-dimensional chemical shift correlation spectra with rotational sidebands in both dimensions are not observed in ^{13}C–^1H spectra at currently available fields and spinning speeds (200–400 MHz for protons, 2–4 kHz spinning speeds). However, at higher fields (500–600 MHz), the proton chemical shift anisotropy will be large enough in some cases that rotational sidebands should be present in both dimensions, even with the scaling factors (~0.5) of the multi-pulse cycles. Furthermore, correlation spectra involving other nuclei with large shift ansiotropies will also exhibit spectra belonging to this class. Some examples might involve correlation of ^{13}C–^{15}N, ^{13}C–^{31}P, or ^{15}N–^{31}P chemical shifts. As in the cases discussed above, the spectra will be useful as assignment aids for both ^{13}C–^1H, ^{13}C–^{15}N, etc. resonances. Similarly, separation of overlapping chemical shift tensors will be facilitated because of the extra spectral dispersion in the second dimension. Moreover, there will be additional information present in the sidebands of these spectra. In particular, the sideband intensities and phases will contain information on the relative orientations of the two shift tensors.[30-32] In Figure 9 we show such a spectrum calculated for two axially symmetric shift tensors in the limit of slow rotation. A dipolar coupling of 30 kHz was assumed, and the coherence transfer was accomplished with the τ–90_l90_s–τ method. The most important feature of this spectrum is the fact that the sideband intensities and phases vary dramatically in both dimensions. By simulating these line shapes the orientation of the two shift tensors may be deduced. The same sort of analysis has been successfully

(30) Munowitz, M. G.; Griffin, R. G.; Bodenhausen, G.; Huang, T. H. *J. Am. Chem. Soc.* **1981**, *103*, 2529.
(31) Munowitz, M. G.; Griffin, R. G. *J. Chem. Phys.* **1982**, *76*, 2848.
(32) Munowitz, M.; Aue, W. P.; Griffin, R. G. *J. Chem. Phys.* **1982**, *77*, 1686.

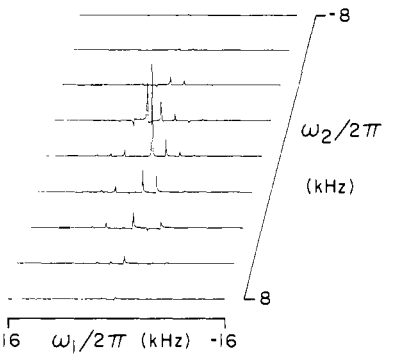

Figure 9. Stacked plot of a calculation employing chemical shift anisotropies of $\Delta\sigma_{^1H}$ = 6 kHz, $\Delta\sigma_{^{13}C}$ = 7.5 kHz, with MASS at 2.0 kHz. The coherence transfer was accompanied with the τ-90_I90_S-τ technique (τ = 20 μs). The heteronuclear dipolar coupling was assumed to be 30 kHz. Note the "phase twists" of some lines; this is a manifestation of the relative orientation of the two chemical shift tensors. See the text for discussion.

employed to determine the relative orientations of shift and dipolar tensors.[31,32]

E. Rotor Frequency Lines. In the course of this work, extra lines were observed in the proton dimension of the 2D spectra. These lines appear at multiples of the spinner speed (0, $\pm\nu_R$, $\pm2\nu_R$, etc.), and their positions are unaffected by varying the resonance offset used during the multiple-pulse sequence. However, the line intensities are strongly offset dependent. Examples of this behavior are illustrated in Figure 10, which shows the effect of changing the proton frequency by 250 Hz in each spectrum (although this appears scaled (by $2^{1/2}/3$) in the figure). The vertical dashed line accentuates the rotor lines at $-\nu_R$. From these and other spectra, it is apparent that these lines "borrow" intensity from the real signal. For the rotor lines to appear, the signal must be near a multiple of ν_R. We note that if this condition is fulfilled, then the rotor lines appear regardless of whether or not there are sidebands in the spectra. These features were first observed in chemical shift scaling experiments,[27,28] where a pulse train is also applied to the spin system being observed during MASS. In another paper it is shown that these extra peaks arise from pulse imperfections, and are a general feature of multiple-pulse/MASS experiments. In particular, computer simulations indicate the rotor lines can be produced by deliberately introducing either pulse length errors or pulse phase errors,[20,33] whereas simulations with perfect pulses do not contain rotor lines.

Summary

The observation of heteronuclear chemical shift correlation spectra in rotating solids opens new avenues for analysis by NMR. The two-dimensional MASS experiment effectively increases the resolution of solid-proton spectra by a factor of 5–10. Since the resolution of ^1H spectra improves approximately linearly with field,[4] it is reasonable to expect that much-improved results will be obtained at yet higher fields (500–600 MHz). In addition, we have investigated several methods for coherence transfer in rotating solids. Although the familiar cross-polarization methods will suffice for some cases, they generally lack the selectivity and efficiency of the single- and multiple-pulse transfer schemes. As is illustrated by the results here, the method chosen for coherence transfer will likely be strongly sample dependent. Thus, in systems with significant motional averaging the single-pulse transfer could be preferred, whereas in rigid solids the simultaneous multiple-pulse experiment appears to be the method of choice. Improvements in both the efficiency and selectivity are clearly desirable. In the course of this work we also observed rotor frequency lines in the proton dimension of the spectra. These lines were noticed

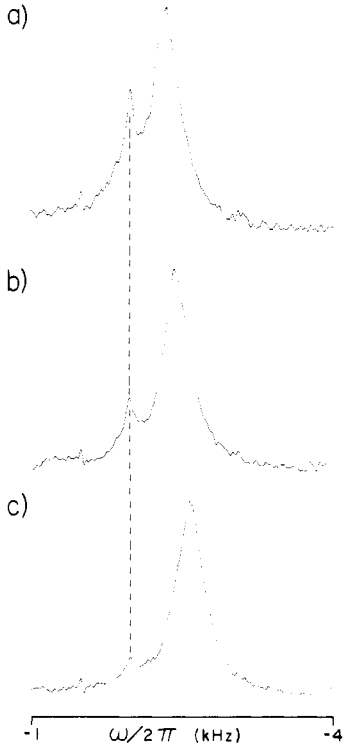

Figure 10. Standard MREV-8 multiple-pulse MASS proton spectra of sodium propionate illustrating a "rotor line" at a multiple of the spinner frequency. The vertical dashed line indicates the rotor line at $-\nu_R$ does not shift as the resonance offset is incremented in steps of 250 Hz. See text for discussion.

previously in chemical shift scaling experiments, and their observation here suggests they are a general feature of multiple-pulse/MASS spectra. Finally, we have discussed the three types of correlation spectra which we believe will be encountered in rotating solids. The first is analogous to that obtained from liquids in that only isotropic resonances will be observed in each dimension. In the second class rotational sidebands will appear in one dimension and the customary shift anisotropies can be extracted from the sideband intensities. In the third class, sidebands will appear in both dimensions and the 2D landscape will contain information on the isotropic and anisotropic chemical shifts as well as data on the relative orientations of the two tensors.

Experimental Section

All experiments were performed on a home-built spectrometer, operating at 317.9 MHz for ^1H and 79.9 MHz for ^{13}C. Radio-frequency field strengths were approximately 25 (^1H) and 60 G (^{13}G), and the multiple-pulse cycle time was typically 48 μs (2 μs pulse, 2 μs τ). The proton frequency was switched on resonance at the start of the detection period to allow for efficient decoupling. Andrew–Beams rotors[34] machined from KEL-F were packed with 50–100 mg of powdered samples; typical spinning rates were 1.5–3.2 kHz. *cis*-Polybutadiene and *p*-dimethoxybenzene were obtained from Aldrich. The sodium propionate sample was 33% by weight of 90% ^{13}C enriched sodium propionate at each of the three carbon positions (Stohler Isotopes).

Acknowledgment. We thank Drs. David Ruben, Malcolm Levitt, Edward Olejniczak, Egbert Menger, and Gerard Harbison for useful discussions during the course of this work. This research was supported by the National Institutes of Health (GM-23403, GM-23289, and RR-00995) and by the National Science Foundation (C-670 and PCM-8216959). J.E.R. is the recipient of a USPHS Postdoctoral Fellowship (GM-09108).

Registry No. Polybutadiene (homopolymer), 9003-17-2; *p*-dimethoxybenzene, 150-78-7; sodium propionate, 137-40-6.

(33) Olejniczak, E. T.; Roberts, J. E.; Vega, S.; Griffin, R. G. *J. Magn. Reson.* **1984**, *56*, 156.

(34) Andrew, E. R.; Farnell, L. F.; Firth, M.; Gledhill, T. D.; Roberts, I. *J. Magn. Reson.* **1964**, *1*, 27.